

Cite this article as: Wang Chunyang, Wang Yuhui, Li Ye, et al. Effect of Texture Inheritance on Microstructure of Beta C Titanium Alloy[J]. Rare Metal Materials and Engineering, 2023, 52(10): 3382-3386.

ARTICLE

Effect of Texture Inheritance on Microstructure of Beta C Titanium Alloy

Wang Chunyang, Wang Yuhui, Li Ye, Zhang Wangfeng

Aviation Key Laboratory of Science and Technology on Advanced Titanium Alloy, AECC Beijing Institute of Aeronautical Materials, Beijing 100095, China

Abstract: The microstructure difference between different parts of the TB9 ingot during hot-working was analyzed, and the microstructure inheritance effect on microstructure evolution and properties of TB9 bar was revealed. The results show that the TB9 ingot can be divided into axial columnar crystal zone at the bottom, equiaxed crystal zone in the core, and columnar crystal zone inclined 45° to the axial direction at the edge. The columnar crystal at the bottom of the ingot with a strong $\langle 100 \rangle$ texture is difficult to break and has a strong heredity, resulting in the residual coarse columnar crystal in corresponding bar after hot rolling, and the tensile strength of the bar after aging is only 987 MPa. The equiaxed crystal zone in the core of the ingot has no obvious preferred orientation, and the corresponding bar after hot rolling has fine equiaxed grains with a tensile strength of 1290 MPa.

Key words: microstructure inheritance; Beta C titanium alloy; texture inheritance; microstructure uniformity

Titanium alloy has been widely used in the aviation field due to excellent characteristics such as low density, high strength and corrosion resistance^[1-2]. Beta C (Ti-3Al-8V-6Cr-4Mo-4Zr) is a metastable β titanium alloy and has good room temperature plasticity and excellent cold workability. The tensile strength of Beta C can reach 1500 MPa with proper process matching, so it is widely used as spring and fastener materials for aircraft^[3-4].

Thermomechanical process is an important processing of titanium alloy from casting ingot to the final product, so deformation behavior of Beta C titanium alloy has been studied extensively^[3-4], so as the metastable β titanium alloy^[5-7]. Research showed that two main texture components with $\langle 110 \rangle$ and $\langle 100 \rangle$ are found in TB6^[5], Ti-5321^[6] and Ti-7333^[7], indicating that thermal deformation can lead to a certain preferred texture. Yan^[8] found that Ti-55531 and other alloys will produce coarse $\langle 100 \rangle$ oriented β grain during thermal thermomechanical process, and inhomogeneous texture of the hot deformed bar from edge to center in cross section is also found in Ti6242^[9] and TC18^[10] alloys, resulting in inhomogeneous microstructure and leading to unstable properties of the final product.

The inhomogeneity microstructure of β titanium alloy is related to the deformation process, but it may also have an

important relationship with the ingot initial structure since the industrial ingot is generally large in size. With the increase in ingot size, the microstructure of different parts of the ingot varies greatly, which may affect the microstructure uniformity of the bar.

Effect of texture inheritance on microstructure and mechanical property of Beta C titanium alloy was studied in this study, which may provide a technical reference for the industrial production of high-quality Beta C titanium alloy rods and wires.

1 Experiment

Mo40V40Al20, AlV85, Al foil, pure Cr, Zr and Ti were used to press the consumable electrode, and then the electrode was vacuum melted four times to $\Phi 440$ mm ingot, with 695 mm in height and 648 kg in mass. The chemical composition of the ingot was Ti-3.8Al-8.0V-5.9Gr-4.2Mo-4.0Zr (wt%).

The lower 1/2 part of the ingot was taken for research as the middle and the bottom of the ingot was located at both ends of the billet during the forging process to ensure that the stress state and cooling conditions at the bottom and middle of the ingot were the same, and thus to eliminate the influence of above factors on the microstructure and mechanical property

Received date: December 27, 2022

Corresponding author: Wang Yuhui, Ph. D., Senior Engineer, Aviation Key Laboratory of Science and Technology on Advanced Titanium Alloy, AECC Beijing Institute of Aeronautical Materials, Beijing 100095, P. R. China, Tel: 0086-10-62496632, E-mail: wyhnoah@126.com

Copyright © 2023, Northwest Institute for Nonferrous Metal Research. Published by Science Press. All rights reserved.

of the bar.

The lower 1/2 part of the ingot was forged by repeated upsetting and drawing above the phase transformation temperature to $\Phi 170$ mm billet. Then it was formed by radial precision forging at 815°C to $\Phi 100$ mm billet, and finally hot rolled to $\Phi 13$ mm bar.

Afterwards $\Phi 100$ mm billet was solution treated at 815°C for 1 h, and then the tensile specimens were taken out at different parts of the billet. The $\Phi 13$ mm bar was solution treated at 815°C for 30 min, and then aged at 480°C for 8 h. The tensile specimens are shown in Fig. 1, and the MTS 810-15 tensile testing machine was used to test the tensile properties. Microstructure phase identification was carried out

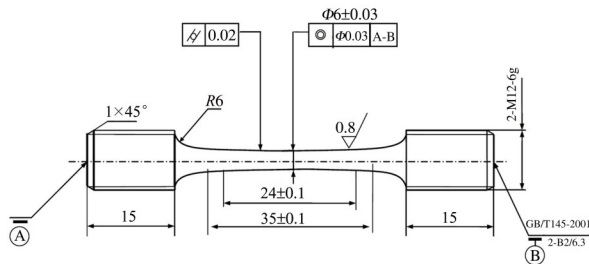


Fig.1 Schematic diagram of tensile specimen

on Smart Lab X-ray diffraction (XRD) with a scanning step of $2^\circ/\text{min}$ from 20° to 90° .

JSM-7001F scanning electron microscope was used to conduct SEM and EBSD analysis. The EBSD microstructure analysis on the axial direction transverse direction (AX-TD) of the sample was conducted with a scanning step of 15, 6, and $3\ \mu\text{m}$ for the ingot, $\Phi 100$ mm billet and $\Phi 13$ mm hot rolled bar.

2 Results and Discussion

2.1 Microstructure of the ingot

Fig. 2a and Fig. 2b show the ingot longitudinal section structure of different parts. The ingot can be divided into shrinkage cavity zone ① at the head of the ingot, equiaxed crystal region ② in the core, equiaxed crystal region ③ at the surface, columnar crystal zone ④ which is inclined 45° to the axial direction, and axial columnar crystal region ⑤ at the bottom. The temperature of the water-cooled crucible is relatively low, and the molten metal will instantly solidify when contacting the crucible, forming a large number of crystal nuclei at external surface of ingot. The molten bath and the water-cooled crucible have a large temperature gradient at the beginning of smelting, so columnar crystal structure forms at the bottom of the ingot. When the distance between the

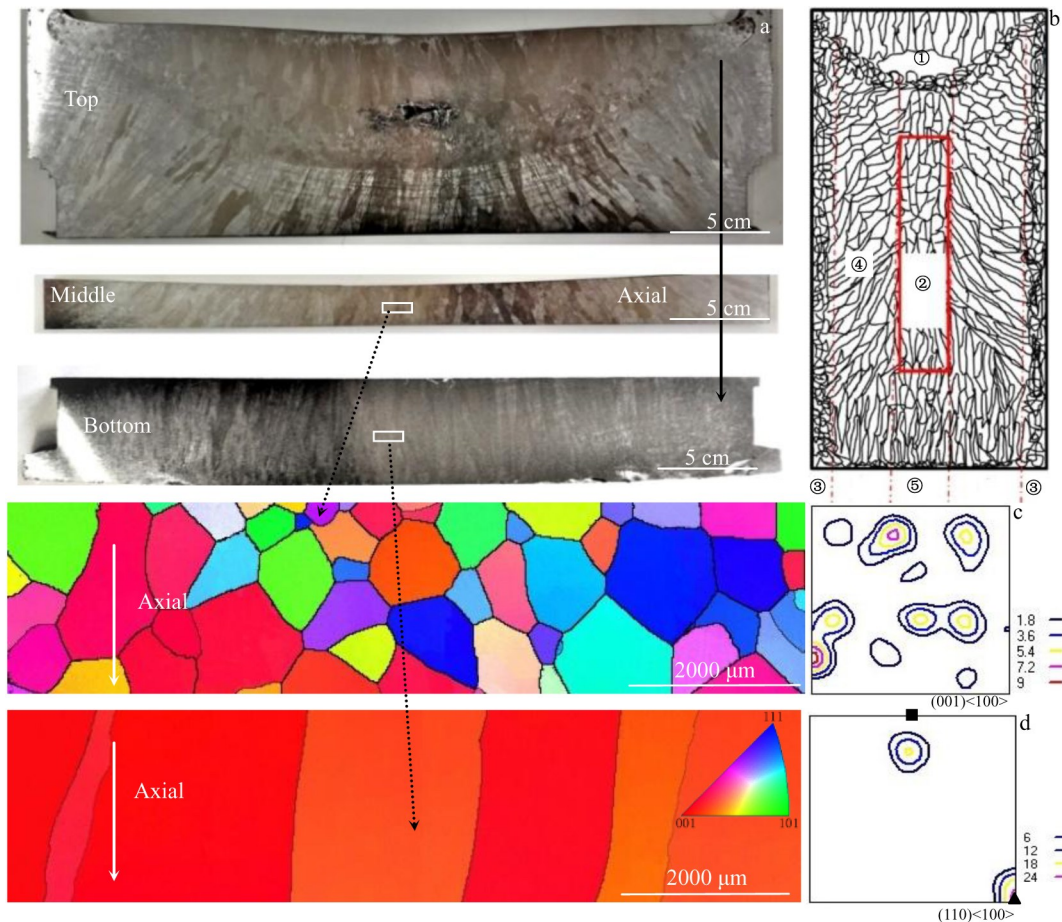


Fig.2 Microstructures of ingot longitudinal section: (a) macroscopic structure, (b) schematic diagram of the ingot microstructure, (c) IPF and ODF ($\varphi_2=45^\circ$) maps of region ②, and (d) IPF and ODF ($\varphi_2=45^\circ$) maps of region ⑤

molten bath and the crucible bottom increases as smelting continues, the molten bath mainly dissipates heat through the crucible sidewall, thus the maximum temperature gradient direction is deflected, and the grain growth direction is also changed, so columnar crystal structure with a certain angle to the axis is formed. The distance of the molten bath from the crucible bottom and the crucible sidewall is large in the middle of the molten bath, and the heat is not easily to be lost, and thus equiaxed crystal region with relatively coarse grains forms in the ingot core.

Fig. 2c and Fig. 2d show the inverse pole figure (IPF) and $\varphi_2=45^\circ$ orientation distribution function (ODF) in region ② and region ⑤. It can be seen that the region ⑤ is mainly composed of strong (110) $\langle 100 \rangle$ texture and (001) $\langle 100 \rangle$ texture, while there is no obvious texture in the equiaxed crystal region ②.

2.2 Texture inheritance of the ingot

Fig. 3 shows the microstructure of $\Phi 100$ mm billet. There is a big spot in the central area of the billet tail, but the outer periphery is fuzzy crystal structure, and the microstructure is

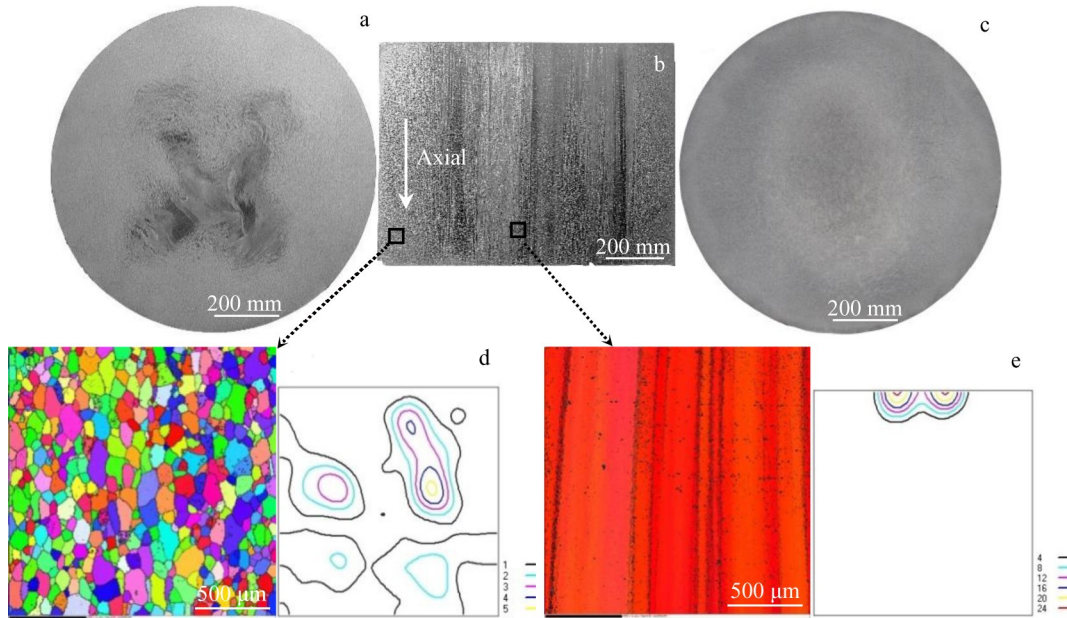


Fig.3 Microstructures of $\Phi 100$ mm billet: (a) cross section of the billet tail, (b) longitudinal section of the billet tail, (c) cross section of the billet head, (d) IPF and ODF ($\varphi_2=45^\circ$) maps of the billet outer periphery, and (e) IPF and ODF ($\varphi_2=45^\circ$) maps of the abnormal microstructure in the core

fibroid along the axial direction in the spot zone (Fig. 3a and Fig. 3b). The macrostructure of the billet tail is extremely inhomogeneous while the macrostructure of the billet head is uniform fuzzy crystal (Fig. 3c).

It can be seen from Fig. 3d that the fuzzy crystal structure consists of equiaxed grains without obvious texture and the highest texture intensity is just only 5. However, the big spot is a large $\{001\} \langle 100 \rangle$ textured columnar grain with a lot of low angle boundaries along the axial direction as shown in Fig. 3e, indicating that the columnar crystal in region ⑤ grows into large columnar grains.

Fig. 4 shows the IPF and ODF diagrams of $\Phi 13$ mm hot-rolled bar. It can be seen that the bar head has a fine equiaxed crystal structure with a grain size about $30 \mu\text{m}$, while there are still part of columnar crystal in the bar tail, although the grains in some areas are obviously refined after hot rolling.

The above research results show that the $\langle 100 \rangle$ textured columnar grain of the ingot has a strong heritability, it is difficult to break during forging and is inherited into the bars. $\langle 100 \rangle$ is a typical compressive texture in metastable β

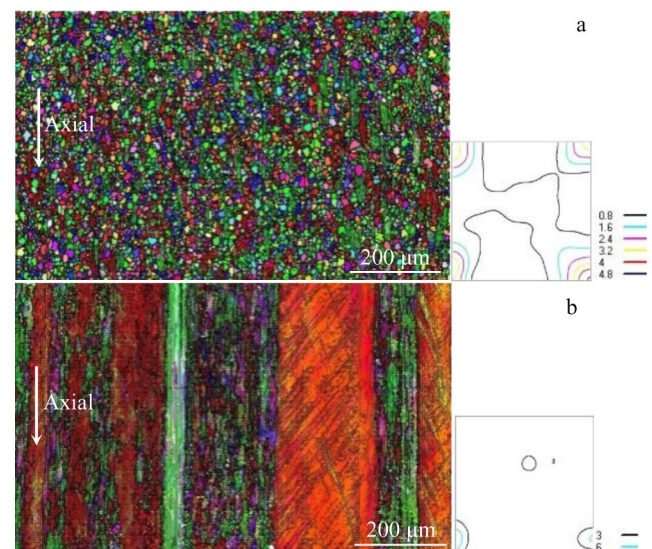


Fig.4 IPF and ODF ($\varphi_2=45^\circ$) maps of the $\Phi 13$ mm hot rolled bar: (a) bar head and (b) bar tail

titanium alloy^[11-12], strengthening of <100> texture is observed for samples deformed at a higher temperature at a low strain rate^[13], thus during upsetting and drawing forging process, the <100> texture is easily formed. In addition, the dynamically recrystallized grains are nucleated at the bulged boundaries and have a similar orientation with respect to the deformed matrix^[14], so many <100> textured dynamically recrystallized grains are formed around the original <100> columnar crystals, and then swallowed by the original <100> columnar crystals, as shown in Fig.5. Thus large {001}<100> textured columnar grain are formed in the billet tail and then inherited into Φ 13 mm hot rolled bar.

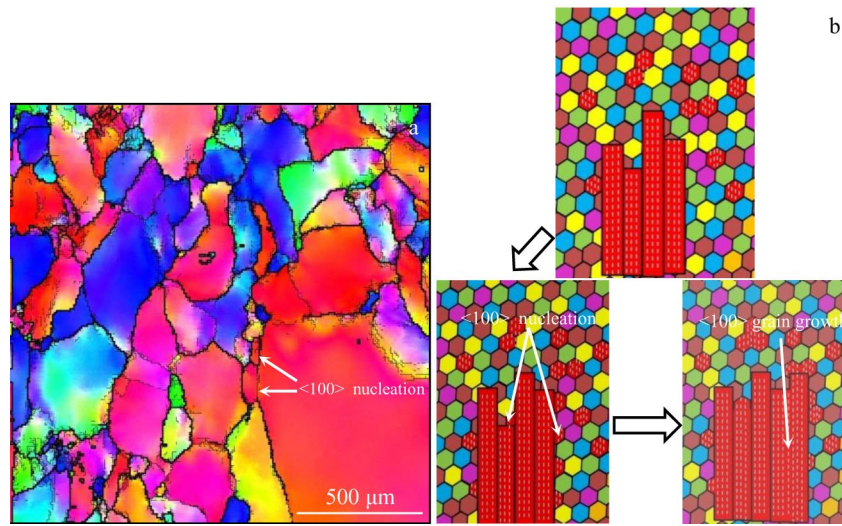


Fig.5 IPF maps of columnar crystal (a) and schematic diagrams of <100> columnar crystal growth (b)

The cooling speed of the Φ 100 mm billet in the central area is slower than the outer periphery, so a small amount of α precipitates are formed during the cooling process, resulting in a decrease in the plasticity of the alloy in the central area with coarse columnar crystals. As shown in Fig.6, α peaks are detected in the central area of the Φ 100 mm billet, whereas it is not found for the outer periphery. Higher α peak is detected in the Φ 13 mm aged bar head, indicating that more α precipitates are formed at the bar head during the aging process.

Fig.7 shows the SEM microstructures of the Φ 13 mm aged bar head. It can be seen that a lot of α precipitates are gathered at the grain boundaries. The above phenomenon is caused by the fact that the α precipitates are mainly formed at the defects and grain boundaries during the aging process^[15-16]. The bar tail made from the columnar crystal area at the bottom of the ingot inherits the columnar crystal structure, and most of the structure is still coarse columnar crystal as shown in Fig.4b. Therefore, the number of α precipitates after aging is less and

Table 1 shows the mechanical properties of the Φ 100 mm billet after solution treatment. Table 2 shows the mechanical properties of the Φ 13 mm hot rolled bar after solution and aging treatment. It can be seen that the tensile strength of the Φ 100 mm billet and Φ 13 mm hot rolled bar is essentially the same at different positions after solution treatment, but the elongation of Φ 100 mm billet in the central area with large {001}<100> textured columnar grain is significantly lower than the former. The tensile strength of the Φ 13 mm hot rolled bar tail is only 987 MPa after aging, while the tensile strength of the bar head is 1290 MPa, which is nearly 45% higher than that of solid solution.

Table 2 Mechanical properties of Φ 13 mm hot rolled bar

Sample	σ_b /MPa	$\sigma_{0.2}$ /MPa	δ_{4D} /%	ψ /%	
Solid solution	Tail	873	850	25.3	61.1
	Head	880	860	25.5	65.1
Solid solution+aging	Tail	987	929	19.0	32.8
	Head	1290.5	1145	13.7	33.7

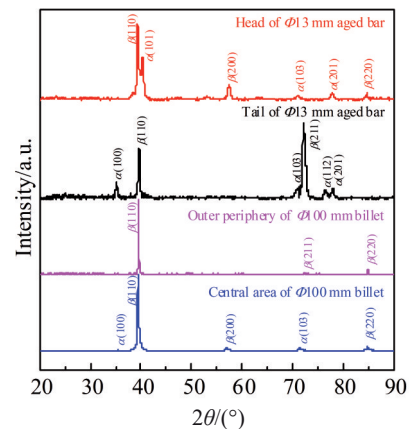


Fig.6 XRD patterns of Φ 100 mm billet after solution and Φ 13 mm aged bar

Table 1 Mechanical properties of Φ 100 mm billet after solution

Sample	σ_b /MPa	$\sigma_{0.2}$ /MPa	δ_{4D} /%	ψ /%
Central area	897	874	15.6	50.8
Outer periphery	890	867	22.4	63.7

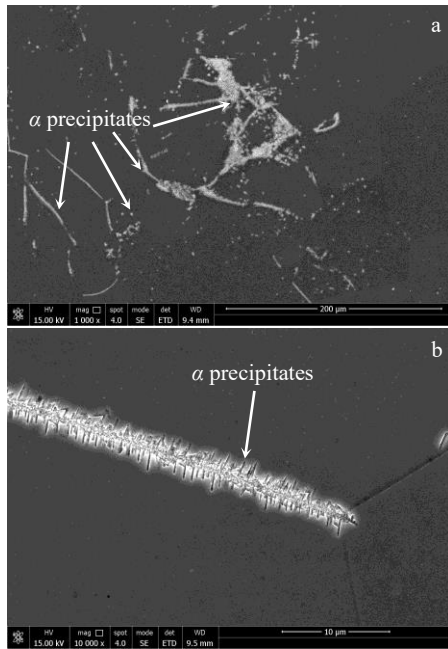


Fig.7 SEM microstructures of the $\Phi 13$ mm aged bar head: (a) 1000X and (b) 10 000X

the tensile strength is only increased by nearly 100 MPa. The bar head made from the equiaxed crystal region of the ingot is mainly fine equiaxed grain as shown in Fig. 4a, and a large amount of α precipitates form at the grain boundaries, so that the strength of the alloy is significantly improved.

3 Conclusions

- 1) The $\langle 100 \rangle$ textured columnar crystal of the Beta C ingot has a strong heredity.
- 2) There is still part of coarse columnar crystal structure in $\Phi 13$ mm bar made from the $\langle 100 \rangle$ columnar crystal zone of the $\Phi 440$ mm ingot, while the bar consists of fine equiaxed grains made from the equiaxed grain zone of the ingot.
- 3) After aging, the tensile strength of columnar crystal

structure is only 987 MPa, while the tensile strength of the equiaxed bar can reach 1290 MPa.

References

- 1 Boyer R R, Briggs R D. *Journal of Materials Engineering and Performance*[J], 2005, 14(6): 681
- 2 Boyer R R. *JOM*[J], 1994, 46: 20
- 3 Nichul U, Khatirkar R, Dhole A et al. *Journal of Alloys and Compounds*[J], 2021, 887(20): 161 400
- 4 Madikizela C, Cornish L A, Chown L H et al. *Materials Science and Engineering A*[J], 2019, 747(18): 225
- 5 Zhu Enrui, Cui Xia, Tao Cheng et al. *Materials Today Communications*[J], 2022, 33: 104 815
- 6 Gu Bing, Chekhonin P, Schaarschuch R et al. *Journal of Alloys and Compounds*[J], 2020, 825(5): 165
- 7 Dong Ruifeng, Zhang Xiaoyang, Li Chenhui et al. *Journal of Materials Science & Technology*[J], 2022, 97: 165
- 8 Yan Mengqi, Zhang Yejin, Li Kai et al. *Chinese Journal of Rare Metals*[J], 2016, 40(6): 534 (in Chinese)
- 9 Zheng Guoming, Mao Xiaonan, Li Lei et al. *Vacuum*[J], 2019, 160: 81
- 10 Li Zhishang, Xiong Zhihao, Yang Ping et al. *Rare Metal Materials and Engineering*[J], 2022, 51(7): 2446 (in Chinese)
- 11 Li Kai, Yang Ping. *Metals*[J], 2017, 7: 412
- 12 Gao Xiongxiang, Zhang Saifei, Wang Lei et al. *Materials Letters*[J], 2021, 301: 130 318
- 13 Fan Jiangkun, Kou Hongchao, Lai Minjie et al. *Materials Science and Engineering A*[J], 2013, 584: 121
- 14 Li Jinshan, Dong Ruifeng, Kou Hongchao. *Materials Characterization*[J], 2019, 159: 109 999
- 15 Ren Dechun, Liu Yujing, Zhang Huibo et al. *Rare Metal Materials and Engineering*[J], 2020, 49(3): 1083 (in Chinese)
- 16 Zhou Xuan, Wang Kelu, Lu Shiqiang et al. *Rare Metal Materials and Engineering*[J], 2021, 50(6): 2155 (in Chinese)

TB9 钛合金棒材组织遗传效应与性能

王春阳, 王玉会, 李 野, 张旺峰

(中国航发北京航空材料研究院 先进钛合金航空科技重点实验室, 北京 100095)

摘要: 以 TB9 钛合金为研究对象, 对比分析了 TB9 铸锭不同部位在热加工过程中的组织差异, 揭示了 TB9 钛合金棒材的组织遗传效应及其对性能的影响。结果表明, TB9 钛合金铸锭可以分为底部沿轴向的柱状晶区, 芯部的等轴晶区, 边部与轴向呈 45° 的柱状晶区。其中铸锭底部的柱状晶具有较强的 $\langle 100 \rangle$ 织构, 在随后的锻造和热轧过程中, $\langle 100 \rangle$ 织构的柱状晶难以破碎, 具有很强的遗传性, 致使最终棒材尾部残留粗大的柱状晶结构, 时效后抗拉强度仅为 987 MPa。铸锭芯部等轴晶区没有明显的择优取向, 最终制备的棒材晶粒细小, 组织均匀, 棒材的性能优良, 抗拉强度可达 1290 MPa。

关键词: 组织遗传; TB9 钛合金; 织构; 组织均匀性

作者简介: 王春阳, 男, 1988 年生, 博士, 中国航发北京航空材料研究院先进钛合金航空科技重点实验室, 北京 100095, 电话: 010-62496632, E-mail: chunyang_2008@163.com